

Optimal entanglement enhancing via conditional measurements

Jiru Liu^{Ⓞ,*}, Yusef Maleki^{Ⓞ,†} and M. Suhail Zubairy[‡]

*Institute for Quantum Science and Engineering (IQSE) and Department of Physics and Astronomy,
Texas A&M University, College Station, Texas 77843-4242, USA*

 (Received 9 February 2022; revised 18 April 2022; accepted 16 May 2022; published 3 June 2022)

Enhancing quantum entanglement is important for many quantum information processing applications. In this paper, we consider a protocol for entanglement enhancing in a two-mode squeezed vacuum state (TMSVS), attained based on photon subtraction, photon catalysis, and photon addition. Central to such an operation is the task of mixing and detecting number states with each mode of TMSVS. We analyze various settings and find an optimal setup for improving the entanglement of the state.

DOI: [10.1103/PhysRevA.105.062405](https://doi.org/10.1103/PhysRevA.105.062405)

I. INTRODUCTION

Among various entangled states, continuous variable (CV) systems have attracted considerable attention for their remarkable characteristics and their usefulness in quantum information tasks [1–5]. Prominent examples of CV systems include both Gaussian and non-Gaussian states. It is well known that Gaussian states, such as coherent and squeezed states, offer a considerable platform for quantum applications. In a parallel line of research, it has been shown that non-Gaussian states, as well as non-Gaussian operations, can play a significant role in quantum information processing. For example, two-mode non-Gaussian states present an advantage over Gaussian states in enhancing entanglement [6–8]. This is an interesting property due to the fact that highly entangled states are of particular importance for both practical applications [9–15] and fundamental investigations in the quantum discipline [13,15,16]. Moreover, non-Gaussian sources are necessary for entanglement distillation since distilling Gaussian states via Gaussian operations is not possible [17,18].

Non-Gaussian states can be obtained by simply adding or subtracting photons to Gaussian states. Photon addition and photon subtraction are important tools for improving quantum correlations. The physical properties of photon-added and photon-subtracted non-Gaussian states are studied both theoretically and experimentally, in recent years [8,19–22]. Photon addition and photon subtraction on squeezing states and the coherent state are used for entanglement distillation [6,23], quantum commutation applications [24,25], and entanglement and teleportation fidelity enhancements [6–8,22,26–32].

Photon subtraction is shown to be realized by taking a small fraction out of the light beam [26,33]. Also, photon addition is demonstrated to be attained in parametric downconversion processes in beta barium borate (BBO) crystals [21]. Both experimental methods include conditional

measurements. Considering these approaches, a similar non-Gaussian operation, photon catalysis, was also studied by Lvovsky and Mlynek [34]. Photon catalysis has been demonstrated to enhance the entanglement of a two-mode squeezed vacuum state [27].

The importance of the non-Gaussian entanglement enhancement recipes that were mentioned earlier becomes more apparent by considering the fact that generating highly entangled states is not an easy task in general and requires delicate control and design of the quantum system [12,15,35]. For example, a two-mode squeezed vacuum state (TMSVS) can be attained using nonlinear crystals [36]. However, due to the weak interaction of nonlinear processes, the squeezing factor is usually small. To be more precise, the entanglement of a TMSVS is determined by $E_N = \log_2 e^{2r}$, where E_N is the logarithmic negativity [37] and r is the squeezing factor.

In this paper, we consider the problem of enhancing the entanglement in TMSVS based on schemes that take advantage of the photon addition, subtraction, and catalysis phenomena. We first analyze and compare the performance of all three operations [27,38]. As demonstrated in Fig. 1, an auxiliary Fock state $|m\rangle_A$ is mixed with one of the modes of a TMSVS via a beam splitter (BS; see Fig. 1). Using a time-multiplexed photon-number-resolving detector [39,40], conditional measurement can be performed on the auxiliary mode of the output states, projecting it to $|m'\rangle_A$. If $m' < m$, this process adds photons to the states, while $m' > m$ subtracts photons from the state. For $m' = m$ it serves as a catalyst. The operation can be performed on both modes of the TMSVS as depicted in Fig. 2, where each mode gets mixed with an independent Fock state. We find that photon catalysis provides better results for both success probability and entanglement enhancement compared with the photon addition and subtraction processes. However, even for the photon catalysis, the success probability of the states does not exceed 20%.

To overcome this limitation and to attain even considerably higher entanglement enhancement, we introduce a different method compared with previous studies [6,7,26,27,29,38]. We show that by injecting the auxiliary Fock states into a BS before mixing them with the modes of the TMSVS, the

*ljr1996@tamu.edu

†maleki@tamu.edu

‡zubairy@physics.tamu.edu

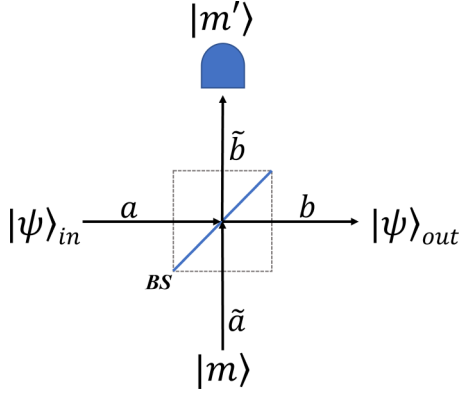


FIG. 1. Quantum state $|\psi\rangle_{out}$ is generated by mixing the Fock state $|m\rangle$ and the input state $|\psi\rangle_{in}$ in the BS, where the state $|m'\rangle$ is detected in the output mode.

entanglement can be drastically improved. With this setup, we demonstrate that under photon addition, the success probability for a large entanglement enhancement can even exceed 70%. Our investigations show that adding a single photon to the TMSVS, based on this protocol, is, in fact, optimal for entanglement enhancement.

II. PHOTON SUBTRACTION, ADDITION, AND CATALYSIS

Now, we consider a general setting of non-Gaussian operations, where photons can be added, subtracted, or catalyzed in the process. The protocol for enhancing entanglement is depicted in Fig. 1, where an input state $|\psi\rangle_{in}$ is injected into one port of a BS and the Fock state $|m\rangle$ is injected into the other port. The BS has the transmittance $T = \cos^2 \theta$. The detector in the output mode detects m' photons, which can be realized using a time-multiplexed photon-number-resolving detector [39,40].

Based on the configurations in Fig. 1, there are three possible scenarios: Photon subtraction for $m' > m$, photon addition for $m' < m$, and photon catalysis for $m' = m$. The BS operation can be described as $\hat{B}(\theta) = \exp\{\theta(a^\dagger a_A - a_A^\dagger a)\}$, where for convenience we take θ to be real and the phase shift of

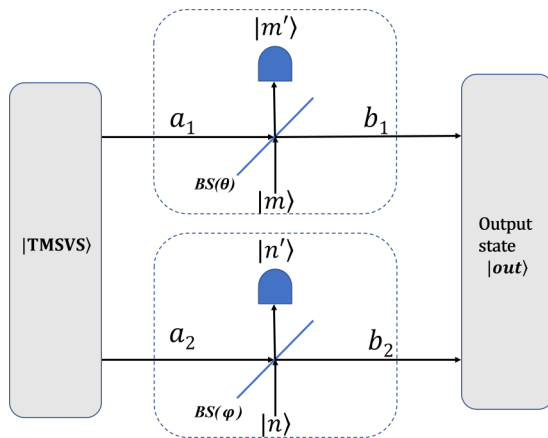


FIG. 2. The two modes of the TMSVS are injected into two BSs separately, generating a two-mode output state $|out\rangle$.

the BS is set to be zero. Together with the photon number measurement operation, the output state $|\psi\rangle_{out}$ is given by

$$|\psi\rangle_{out} = {}_A \langle m' | \hat{B}(\theta) | m \rangle_A |\psi\rangle_{in}, \quad (1)$$

where index A denotes the auxiliary mode. Note that the BS operator consists of two modes and hence ${}_A \langle m' | \hat{B}(\theta) | m \rangle_A$ is an operator acting on the mode that is not measured. Thus the transformation from $|\psi\rangle_{in}$ to $|\psi\rangle_{out}$ is expressed by

$$\begin{aligned} |\psi\rangle_{out} &= \hat{B}_{m,m'} |\psi\rangle_{in}, \\ \hat{B}_{m,m'} &= {}_A \langle m' | \hat{B}(\theta) | m \rangle_A. \end{aligned} \quad (2)$$

Considering Eq. (2), in order to determine the output state, we need to determine $\hat{B}_{m,m'}$. As is shown in the Appendix, the operator $\hat{B}_{m,m'}$ can be expressed in the Fock basis through

$$\hat{B}_{m,m'} = {}_A \langle m' | \hat{B}(\theta) | m \rangle_A = \sum_{k=0} B_{m,m',k} |k + m - m'\rangle \langle k|, \quad (3)$$

where the explicit expression for the coefficient $B_{m,m',k}$ is presented in Eq. (A3), in the Appendix. This provides a rather general framework for non-Gaussian operations on a quantum state.

To consider a particular setting, for the input state $|\psi\rangle_{in} = \sum_k c_k |k\rangle$, the output state $|\psi\rangle_{out}$ can be obtained to be

$$|\psi\rangle_{out} \propto \hat{B}_{m,m'} |\psi\rangle_{in} = \sum_{k=0} c_k B_{m,m',k} |k + m - m'\rangle. \quad (4)$$

Note that $\hat{B}_{m,m'} |\psi\rangle_{in}$ is not normalized in general. Therefore, considering the normalized factor $N_{m,m'}$, determined by $N_{m,m'}^{-2} = \sum_k |c_k B_{m,m',k}|^2$, the output state can be expressed as

$$|\psi\rangle_{out} = N_{m,m'} \sum_{k=0} c_k B_{m,m',k} |k + m - m'\rangle. \quad (5)$$

As a particular example, for the photon catalysis with $m = m' = 1$, we find for the output state

$$|\psi\rangle_{out} = N_{1,1} \sum_{k=0} c_k (\cos \theta)^{k-1} [\cos^2 \theta - k \sin^2 \theta] |k\rangle, \quad (6)$$

which agrees with Refs. [27,41,42]. Taking into account the fact that $T = \cos^2 \theta$ and $R = \sin^2 \theta$, the equation above can be expressed as $|\psi\rangle_{out} = N_{1,1} \sum_{k=0} c_k \sqrt{T}^{k-1} [T - kR] |k\rangle$. Therefore, for $k = T/R$, the contribution from the Fock state $|k\rangle$ becomes eliminated in the output state. As a specific case, for $|\psi\rangle_{in} = |k\rangle$, we obtain $|\psi\rangle_{out} = 0$. For a given state, if we take $T = R$, for instance, there will be no contribution from the number state $|1\rangle$ in the output. For $T = 2R$ there will be no contribution from the number state $|2\rangle$ in the output state, for instance.

III. ENTANGLEMENT ENHANCEMENT OF THE TMSVS

Now that we have developed a platform for desired non-Gaussian operations, we can implement specific setups for enhancing entanglement in a continuous variable system. Even though the input state introduced in Fig. 1 is quite general, we apply the quantum enhancement protocols to the two-mode squeezed vacuum state (TMSVS). The two-mode squeezed vacuum state is defined by applying two-mode

squeezing operator $S(r) = \exp\{r(a_1^\dagger a_2^\dagger - a_1 a_2)\}$ to the two-mode vacuum state $|0, 0\rangle$ as [27,41,42]

$$|\text{TMSVS}\rangle = S(r)|0, 0\rangle = \text{sechr} \sum_{k=0} \lambda^k |k, k\rangle, \quad (7)$$

where $\lambda = \tanh r$ (for convenience, r is set to be real). The operators $a_1^\dagger(a_1)$ and $a_2^\dagger(a_2)$ are the creation (annihilation) operators for the two modes.

In particular, we consider two different setups for entanglement enhancements and determine the optimal scenario to achieve the goal.

A. First setup

Now, we introduce the first scheme for the enhancement of the entanglement in the TMSVS. The setup is presented in Fig. 2, where each mode goes through the operation that is explained in Fig. 1. Considering the formalism developed in the previous section, the output state is given by

$$\begin{aligned} |\text{out}\rangle &= N_{m,m':n,n'} \hat{B}_{m,m'}(\theta) \hat{B}_{n,n'}(\varphi) |\text{TMSVS}\rangle \\ &= N_{m,m':n,n'} \sum_{k=0} C_{m,m':n,n',k} |k+m-m', k+n-n'\rangle, \end{aligned} \quad (8)$$

where $C_{m,m':n,n',k}$ is the coefficient of $|k+m-m', k+n-n'\rangle$. Note that $N_{m,m':n,n'}$ is the normalization factor such that $\langle \text{out} | \text{out} \rangle = 1$. $C_{m,m':n,n',k}$, which we denote as C_k for convenience, can be obtained using the two separate non-Gaussian operations operated on each mode. In this setting, we have $C_k = \text{sechr} \lambda^k B_{m,m',k}(\theta) B_{n,n',k}(\varphi)$.

In this operation, the success probability and the entanglement enhancement are the two quantities that determine how useful the operation outcome is. $N_{m,m':n,n'}^{-2}$ quantifies the success probability of the conditional measurement $m \rightarrow m'$ and $n \rightarrow n'$, which is determined by $N_{m,m':n,n'}^{-2} = \sum_{k=0} |C_k|^2$. For quantifying entanglement, we use the logarithmic negativity E_N as a measure of entanglement which is given by [37]

$$E_N(\rho) = \log_2 \|\rho^{T_A}\|_1, \quad (9)$$

where $\|R\|_1$ denotes the trace norm $\text{Tr}\sqrt{R^\dagger R}$ and ρ^{T_A} is the partial transpose of the state ρ . In Eq. (8), $|\text{out}\rangle$ is in a Schmidt form, for which the logarithmic negativity is given by

$$E_N = \log_2 \left[N_{m,m':n,n'}^2 \left(\sum_{k=0} |C_k| \right)^2 \right]. \quad (10)$$

This formulation clearly shows that the entanglement is determined by the coefficient norms $|C_k|$. Considering the explicit form of the coefficients as $C_k = \text{sechr} \lambda^k B_{m,m',k}(\theta) B_{n,n',k}(\varphi)$, it is evident that the characteristics of the beam splitters and also m, m', n , and n' determine the entanglement. In general, the entanglement can be increased or decreased for some specific parameters. However, the interesting scenario is to find the parameter space where the entanglement increases.

The initial entanglement for TMSVS, whose Schmidt form is shown by Eq. (7), can be calculated from Eq. (10), which results in $E_N(\text{TMSVS}) = 2r \log_2 e$. Therefore the entanglement change is determined by

$$\Delta E_N = \log_2 \left[N_{m,m':n,n'}^2 \left(\sum_{k=0} |C_k| \right)^2 \right] - 2r \log_2 e. \quad (11)$$

This relation is central to the investigation of the entanglement improvement by the protocol. In fact, if E_N is positive, then we can conclude that the entanglement has increased. To find the parameter space in which entanglement can be enhanced, we consider various settings and identify the cases in which entanglement can be enhanced more efficiently. To be more specific, we compare the enhancement for photon addition, subtraction, and catalysis and determine which operation can increase the entanglement better.

In some of the recent studies, photon subtraction (addition) is implemented by directly applying an annihilation (creation) operator to the input state, and the theoretical analysis is based on the normalized state $\hat{a}|\psi\rangle_{\text{in}}, \hat{a}^\dagger|\psi\rangle_{\text{in}}$ and the coherent superposition $(t\hat{a} + r\hat{a}^\dagger)|\psi\rangle_{\text{in}}$ [6,7,19,43,44]. Our scheme in Fig. 1 adds or subtracts photons or operates photon catalysis using a beam splitter and a conditional measurement. The analysis and simulation are based on the output state $|\psi\rangle_{\text{out}}$ given by Eq. (5).

We plot the outcome for the three operations for the case with $m = 1$ in Fig. 3. In this figure, for convenience and without loss of generality, no operations are applied to the lower mode of the TMSVS. For photon addition [Figs. 3(a) and 3(b)], $m' = 0$, one photon is added to the TMSVS. As is shown in Fig. 3(b), there is no entanglement enhancement in the whole parameter space in this case. Therefore such a photon addition is not useful for entanglement improvements. For photon subtraction [Figs. 3(e) and 3(f)], $m' = 2$, one photon is subtracted from the TMSVS. As we can see from Fig. 3(e), this operation has a quite small success probability in the regions where entanglement can be enhanced.

Photon catalysis with $m' = 1$ is shown in Figs. 3(c) and 3(d). These plots show that the entanglement can be enhanced using a catalysis setting. However, the entanglement enhancement regions in Fig. 3(d) correspond to the regions with the low success probability in Fig. 3(c). Nevertheless, the entanglement enhancement in this case is better than both the photon addition and the photon subtraction settings [27]. It is worth mentioning that, even though we presented the $m = 1$ scenario in Fig. 3, this finding is true beyond this specific case, where one can consider larger m and various numbers of photons detected in the output mode. Therefore our study unifies the previous consideration in the literature in a comparative setting and shows how various proposals can be compared with each other. Even though we observe that photon catalysis is a better route to quantum entanglement enhancement compared with the two other cases, in the Fig. 2 framework, the outcome still is not very compelling due to the low success probabilities. To overcome this limitation, we propose a different protocol enabling much higher success probabilities and large entanglement enhancements in Sec. III B.

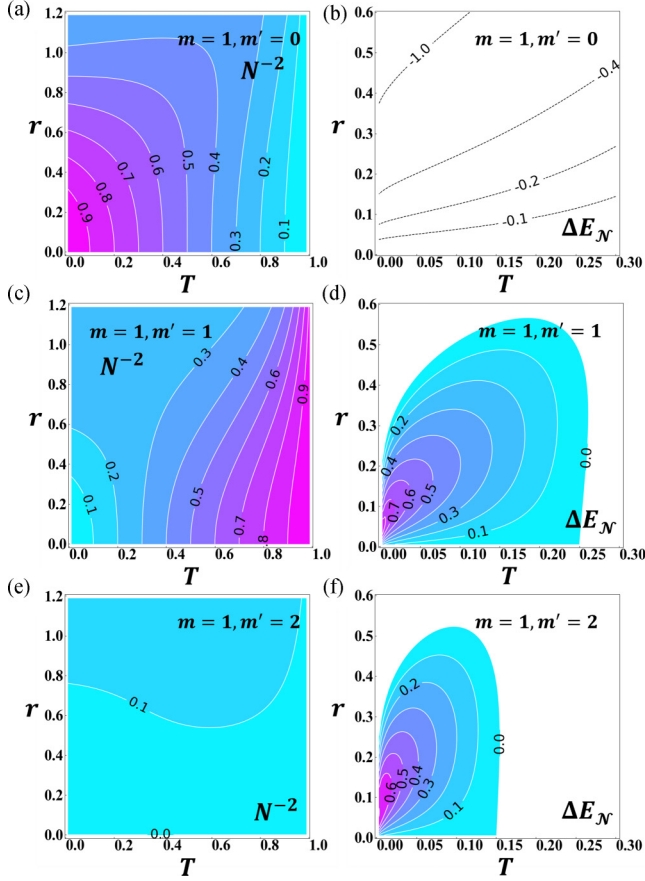


FIG. 3. The three operations for $m = 1$. (a) and (b) Photon addition. (c) and (d) Photon catalysis. (e) and (f) Photon subtraction. (a), (c), and (e) present the success probability vs the squeezing factor r and the transmittance $T = \cos^2 \theta$, while (b), (d), and (f) show the entanglement enhancement for different cases.

B. Second setup

Now, we introduce a method for increasing entanglement that is different from the one depicted in Fig. 2. We already considered the three non-Gaussian operations on the TMSVS where each mode undergoes a separate operation, using the product Fock states $|m\rangle \otimes |n\rangle$ as auxiliary states. Among these schemes, we found that photon catalysis has the best success probability as well as entanglement improvement compared with photon addition and subtraction. However, according to Figs. 3(c) and 3(d), for a suitable r and T , the region which corresponds to a considerable entanglement enhancement has a moderately low success probability that is approximately less than 20%.

We show that a slight adjustment in the setup can drastically enhance both the entanglement and the success probability. This adjustment requires an extra BS (BS_A), as is shown in Fig. 4. In this setting, the auxiliary input states for each mode first undergo BS_A before the operation of Fig. 2 is performed. This process can entangle the two auxiliary modes and finally apply the non-Gaussian operations to the modes of the TMSVS [22,45]. Since this extra step is unitary, no photon is lost in this process. This extra step is not challenging to implement in the experiment due to the simplicity of BS

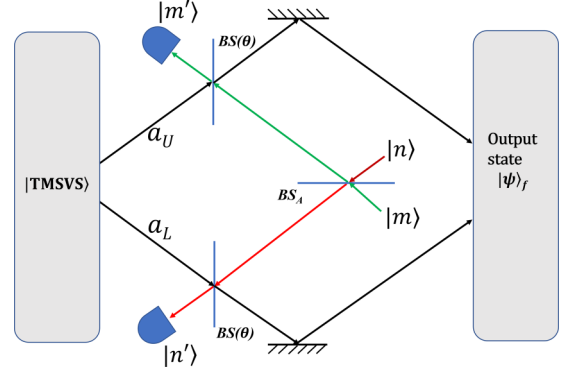


FIG. 4. A similar setting to Fig. 2, but the auxiliary states are first mixed via BS_A before the operations are carried out on the TMSVS.

operations in general. Therefore any improvement attained in the process can be useful in a practical setting.

In Fig. 4, we simplify the auxiliary input source to one single-photon state ($m = 1, n = 0$). Once $|\psi\rangle_A$ is mixed with the TMSVS via $BS(\theta)$, the conditional detection of $|00\rangle_A$ ($m' = 0, n' = 0$) adds one photon to the TMSVS.

For $m = 1, n = 0$, before BS_A , the entire state is

$$\begin{aligned}
 |\psi\rangle_i &= \text{sechr} \sum_{k=0} \lambda^k |k\rangle_U |k\rangle_L |1\rangle_{UA} |0\rangle_{LA} \\
 &= \text{sechr} \sum_{k=0} \lambda^k a_{UA}^\dagger |kk\rangle_{|00\rangle_A} \\
 &= \text{sechr} \sum_{k=0} \frac{\lambda^k}{k!} (a_U^\dagger)^k (a_{UA}^\dagger) (a_L^\dagger)^k |00\rangle_{|00\rangle_A}, \quad (12)
 \end{aligned}$$

where the creation operator of the upper TMSVS mode is denoted as a_U^\dagger while the lower one is denoted as a_L^\dagger . Moreover, the creation operator for the upper path (shown in green) of the ancillary state in Fig. 4 is denoted as a_{UA}^\dagger , while the lower one (shown in red) is a_{LA}^\dagger . In the second step of the above equations, $|ij\rangle_A$ stands for $|i\rangle_{UA} |j\rangle_{LA}$, and $|ij\rangle$ is simply the basis for the two modes of the TMSVS, $|i\rangle_U |j\rangle_L$.

After passing through BS_A , we attain $|\psi\rangle_1$. This state, when it passes through BS_U and BS_L , degenerates to $|\psi\rangle_2$, where $|\psi\rangle_1$ and $|\psi\rangle_2$ are given by

$$\begin{aligned}
 |\psi\rangle_1 &= \frac{1}{\sqrt{2}} \text{sechr} \sum_{k=0} \frac{\lambda^k}{k!} (a_U^\dagger)^k (a_{UA}^\dagger + a_{LA}^\dagger) (a_L^\dagger)^k |00\rangle_{|00\rangle_A}, \\
 |\psi\rangle_2 &= \frac{1}{\sqrt{2}} \text{sechr} \sum_{k=0} \frac{\lambda^k}{k!} (b_U^\dagger)^k (b_{UA}^\dagger + b_{LA}^\dagger) (b_L^\dagger)^k |00\rangle_{|00\rangle_A}. \quad (13)
 \end{aligned}$$

Here, $b^\dagger = \cos \theta a^\dagger + \sin \theta a_A^\dagger$ and $b_A^\dagger = -\sin \theta a^\dagger + \cos \theta a_A^\dagger$. Note that b^\dagger denotes b_U^\dagger or b_L^\dagger while b_A^\dagger denotes b_{UA}^\dagger or b_{LA}^\dagger .

In principle, detecting $m' = 0, n' = 0$ leads to one photon addition to the TMSVS. Substituting b_L^\dagger, b_U^\dagger and $b_{UA}^\dagger, b_{LA}^\dagger$ into

the expression of $|\psi\rangle_2$, it follows that

$$\begin{aligned}
|\psi\rangle_f &= N {}_A\langle 00|\psi\rangle_2 \\
&= N \frac{\text{sechr}}{\sqrt{2}} \sum_{k=0}^{\infty} \frac{\lambda^k}{k!} (\cos\theta a_U^\dagger)^k (\cos\theta a_L^\dagger)^k \\
&\quad \times (-\sin\theta a_U^\dagger - \sin\theta a_L^\dagger)|00\rangle \\
&= N \frac{\text{sechr}}{\sqrt{2}} \sum_{k=0}^{\infty} (\lambda \cos^2\theta)^k (-\sin\theta a_U^\dagger - \sin\theta a_L^\dagger)^k |kk\rangle \\
&= -N \frac{\text{sechr}}{\sqrt{2}} \sum_{k=0}^{\infty} (\lambda \cos^2\theta)^k \sin\theta \sqrt{k+1} [|k+1, k\rangle \\
&\quad + |k, k+1\rangle], \tag{14}
\end{aligned}$$

where N is the normalized factor.

Up to an unimportant global phase, and for $\theta \neq 0$, the state at the output can be expressed as

$$|\psi\rangle_f = (1 - \lambda^2 \cos^4\theta) \sum_{k=0}^{\infty} [(\lambda \cos^2\theta)^k \sqrt{k+1}] |\phi\rangle_k, \tag{15}$$

where $|\phi\rangle_k = \frac{1}{\sqrt{2}}(|k+1, k\rangle + |k, k+1\rangle)$. Alternatively, we can write the state as $|\psi\rangle_f = \sum_{k=0}^{\infty} \sqrt{p_k} |\phi\rangle_k$, in which p_k is the probability of having the state $|\phi\rangle_k$ given by $p_k = (1 - \lambda^2 \cos^4\theta)^2 (\lambda \cos^2\theta)^{2k} (k+1)$. The state $|\phi\rangle_k$ is a maximally entangled state with any k . Therefore the output state $|\psi\rangle_f$ reduces to superposition of different maximally entangled states with the probability determined by p_k . An interesting observation is to find which entangled state ($|\phi\rangle_k$) is most probable given the probability distribution p_k . To this end, one can easily find $p_{k+1}/p_k = (\lambda^2 \cos^4\theta)(k+2)/(k+1)$. When the squeezing factor r is small enough ($\lambda = \tanh r$), we have $p_{k+1}/p_k < 1$. Therefore the most probable state can be attained for $k=0$, i.e., $|\phi\rangle_0 = (|1, 0\rangle + |0, 1\rangle)/\sqrt{2}$. However, for the case when $2\lambda^2 \cos^4\theta > 1$, one can determine the peak in the probability distribution by setting $p_{k+1} = p_k$. This gives $k = [1/(1 - \lambda^2 \cos^4\theta)] - 2$.

The output state for photon catalysis and photon subtraction can be obtained by applying ${}_A\langle 10|$ (or ${}_A\langle 01|$) and ${}_A\langle 11|$ to $|\psi\rangle_2$, respectively.

The success probability as well as the entanglement enhancement can be calculated from Eq. (14). It is worth mentioning that, for $|\psi\rangle_2$ in the last step of Eq. (14), we apply Schmidt decomposition to $|\psi\rangle_f$ to get the singular eigenvalue C_k and then use Eqs. (10) and (11) to obtain the entanglement enhancement.

In Fig. 5 we present the photon addition operation for the protocol presented Fig. 4. In Fig. 5 we have $m=1, n=0$, and $m'=n'=0$. Therefore the detectors do not click in this case, i.e., the detected state is $|00\rangle_A$. Figure 5(a) presents the success probability varying with squeezing factor r and $T = \cos^2\theta$, while Fig. 5(b) shows the enhancement entanglement.

Compared with Fig. 3, there is a considerable improvement in both success probability and entanglement with the same resources ($m=1, n=0$, and $m'=n'=0$). An interesting observation is that in the configuration of Fig. 4, photon catalysis does not provide a better result compared with photon

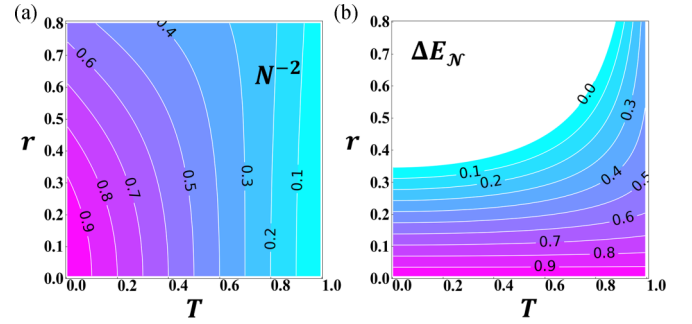


FIG. 5. Photon addition operation for detecting $|00\rangle_A$ in the protocol presented in Fig. 4. In other words, $m=1, n=0$, and $m'=n'=0$. (a) is the success probability varying with squeezing factor r and $T = \cos^2\theta$, while (b) is the entanglement enhancement.

addition. Instead, the single-photon addition with this process shows a much better outcome when compared with the settings from the previous setup. Therefore the protocol in Fig. 4 provides a better route for entanglement enhancing using beam splitters and photon detection operations. This observation improves the previous efforts for enhancing the entanglement of the TMSVS in Refs. [27,41,42].

Considering the setup in Fig. 2, the entanglement enhancement of the state by photon catalysis, obtained from the TMSVS, is shown to be higher than that of the photon-subtracted and photon-added state [27], which is in agreement with the observations of this paper. In multimode squeezing state, the superiority of photon subtraction to photon addition has been reported [46]. However, our investigations for the TMSVS show that photon addition performs better than either photon subtraction or photon catalysis.

We also note that one might assume that the existence of the entanglement in the auxiliary modes, after BS_A , is the reason for the better performance in this setting. However, this might not necessarily be the case. To illustrate this, we consider the setting $m=1, n=1$, for which the entangled state after passing through BS_A is $|\psi\rangle_A = \frac{1}{\sqrt{2}}(-|20\rangle_A + |02\rangle_A)$, which is a maximally entangled state [47]. However, the result of such a process is not as good as what we can get in Fig. 4. Specific settings are presented in Fig. 6 by way of illustration. As is shown in Figs. 6(a) and 6(c), the success probabilities are much lower than the result in Fig. 5(a). Therefore it is not proper to assume that the entanglement from the auxiliary modes is “transmitted” to the TMSVS. As a result, single-photon addition through the setup given in Fig. 4 provides an optimal enhancement in the entanglement of a TMSVS. We in fact analyzed several different settings beyond the scope of Fig. 6; however, none of the scenarios provides a better result than what we presented in Fig. 5. Therefore the desirable method for enhancing entanglement seems to be the setting used in Fig. 5.

An appealing feature of our optimal quantum entanglement in the second setup is that it does not require high-number Fock states. Basically, we only need a single-photon input state and dark detection in the detectors, as is analyzed in Fig. 5. Even the scenario described in Fig. 6 does not rely on high-number Fock states. In Figs. 6(a) and 6(b), for photon catalysis with the $|10\rangle$ auxiliary state, the

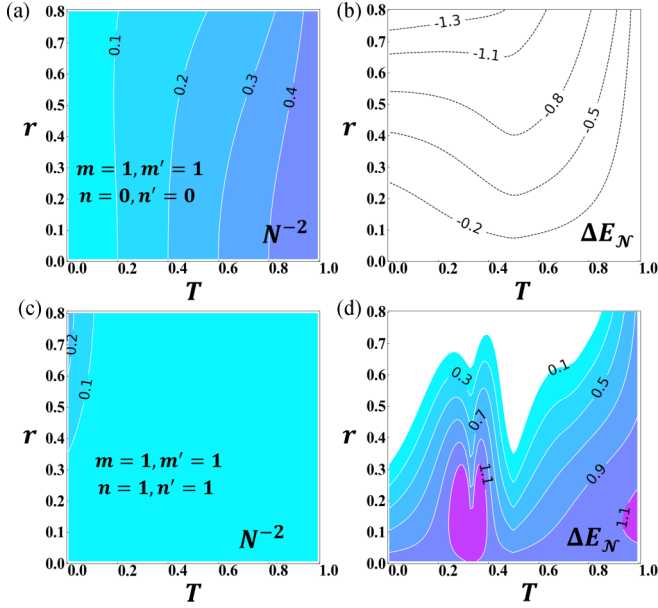


FIG. 6. (a) Success probability and (b) entanglement enhancement for photon catalysis for a single-photon auxiliary source ($m = 1$, $n = 0$) and conditionally detecting $m' = 1$, $n' = 0$. (c) Success probability and (d) entanglement enhancement for photon catalysis for an ancillary source $m = 1$, $n = 1$ and conditionally detecting $m' = 1$, $n' = 1$.

detected state is $|10\rangle$. Similarly, in Figs. 6(c) and 6(d), for photon catalysis with the $|11\rangle$ auxiliary state, the detected state is $|11\rangle$.

The optimal situation, which requires a single-photon source as auxiliary input and detecting zero photons, provides another advantage from the photon detection point of view. Considering the fact that the dark counts of a single-photon avalanche detector (SPAD) can be as low as 50 per second while the weak photon signal reads as high as 10^4 per second [48–50], ensuring that a no-photon event can conveniently be distinguished from single-photon Fock states. Also, the detection of high-number Fock states is more challenging in general, while our proposed scenario does not rely on that. The conditional measurements can be done just with a single-photon detector, which simplifies the detection processing as well as improves the detection accuracy.

Besides the photon detection error, the other imperfection may be accumulated from the BSs. Since the existing BSs are highly efficient in realistic experiments, the error in BSs can usually be neglected. In fact, systems containing even a network of many BSs have intensively been considered in the literature. In this paper, there is no need for a high number of BSs, and thus the imperfections cannot impair the performance of the protocols.

IV. SUMMARY AND CONCLUSION

In this paper, we considered a protocol for entanglement enhancing in a TMSVS based on photon subtraction, photon catalysis, and photon addition. Central to such an operation

is the task of mixing and detecting number states with each mode of the TMSVS and nondeterministic detection. We analyzed various settings for the improvement of quantum entanglement and found an optimal setup for enhancing the entanglement of the state. To be more specific, we considered two different schemes for enhancing entanglement. In the first scheme each mode interacts with a Fock state in a beam splitter. In the second scheme, Fock states undergo a beam splitter before interacting with the modes of the TMSVS.

In the first scheme, photon catalysis outperforms both photon addition and subtraction operations. Nonetheless, the improvement and the success probability remain rather low even for photon catalysis. Of course, entanglement, in this case, can be improved more by using higher-number Fock states for resources. However, generating as well as detecting a high-number Fock state $|m\rangle$ is quite challenging.

In contrast to the first scheme, it turns out that the optimal performance of the second setup can be achieved simply using single-photon sources. This, in fact, simplifies both photon generation and detection processes from a practical point of view. The optimal scenario presented in this paper can drastically outperform all the settings of the first scheme, with a more than threefold improvement of the entanglement.

Quantum entanglement improvement based on non-Gaussian operations has been investigated from various perspectives in recent years [8,19–22,34]. Such operations are shown to be useful for entanglement distillation [6,23], quantum commutation [24,25], and quantum teleportation [8,22,26,27]. Therefore the optimal entanglement enhancement proposed here can provide an important tool for such applications.

ACKNOWLEDGMENTS

This research is supported by Project No. NPRP 13S-0205-200258 of the Qatar National Research Fund (QNRF). J.L. is supported by the HEEP Graduate Fellowship.

APPENDIX: DERIVATION OF $\hat{B}_{m,m'}$

The BS operator $\hat{B}(\theta)$ performs a transformation to the input modes by

$$\begin{aligned} b_A^\dagger &= \hat{B}(\theta) a_A^\dagger \hat{B}(\theta)^\dagger = \cos \theta a_A^\dagger + \sin \theta a^\dagger, \\ b^\dagger &= \hat{B}(\theta) a^\dagger \hat{B}(\theta)^\dagger = -\sin \theta a_A^\dagger + \cos \theta a^\dagger. \end{aligned} \quad (\text{A1})$$

From Eq. (2), in order to determine the output state, we need to compute $\hat{B}_{m,m'}$.

$$\begin{aligned} \hat{B}_{m,m'} &= {}_A \langle m' | \hat{B}(\theta) | m \rangle_A = {}_A \langle m' | \hat{B}(\theta) \sum_{k=0}^{\infty} |m\rangle_A |k\rangle \langle k| \\ &= {}_A \langle m' | \sum_{k=0}^{\infty} \hat{B}(\theta) (a_A^\dagger)^m (a^\dagger)^k \frac{1}{\sqrt{m!}} \frac{1}{\sqrt{k!}} |0\rangle_A |0\rangle \langle k| \\ &= {}_A \langle m' | \sum_{k=0}^{\infty} (b_A^\dagger)^m (b^\dagger)^k \frac{1}{\sqrt{m!}} \frac{1}{\sqrt{k!}} |0\rangle_A |0\rangle \langle k| \\ &= \sum_{k=0}^{\infty} B_{m,m',k} |k+m-m'\rangle \langle k|. \end{aligned} \quad (\text{A2})$$

Considering ${}_A\langle m'|$, which is inserted from the measurement, the nonzero term must contain $(a_A^\dagger)^{m'}|0\rangle$. Substituting the expressions for b_A^\dagger and b^\dagger from Eq. (A1) into Eq. (A2), we have

$$\begin{aligned}\hat{B}_{m,m'} &= {}_A\langle m'| \sum_{k=0} (\cos\theta a_A^\dagger + \sin\theta a^\dagger)^m (-\sin\theta a_A^\dagger + \cos\theta a^\dagger)^k \frac{1}{\sqrt{m!}} \frac{1}{\sqrt{k!}} |0\rangle_A |0\rangle \langle k| \\ &= {}_A\langle m'| \sum_{k=0} \sum_{i=0}^{m'} \binom{m}{i} (\cos\theta)^i (\sin\theta)^{m-i} \binom{k}{m'-i} (-\sin\theta)^{m'-i} (\cos\theta)^{k+i-m'} (a_A^\dagger)^{m'} (a^\dagger)^{m+k-m'} \frac{1}{\sqrt{m!}} \frac{1}{\sqrt{k!}} |0\rangle_A |0\rangle \langle k| \\ &= \sum_{k=0} \sum_{i=0}^{m'} (-1)^{m'-i} \binom{m}{i} \binom{k}{m'-i} (\cos\theta)^{k+2i-m'} (\sin\theta)^{m+m'-2i} \frac{\sqrt{m!}}{\sqrt{m!}} \frac{\sqrt{(k+m-m')!}}{\sqrt{k!}} |k+m-m'\rangle \langle k| \\ &= \sum_{k=0} B_{m,m',k} |k+m-m'\rangle \langle k|,\end{aligned}$$

$$\text{with } B_{m,m',k} = \sum_{i=0}^{m'} (-1)^{m'-i} \binom{m}{i} \binom{k}{m'-i} (\cos\theta)^{k+2i-m'} (\sin\theta)^{m+m'-2i} \frac{\sqrt{m!}}{\sqrt{m!}} \frac{\sqrt{(k+m-m')!}}{\sqrt{k!}}. \quad (\text{A3})$$

Note that $\binom{a}{b} = 0$ if $a < b$, thus, the situation when $m' > m$ or $m' < m$, $m' > k$ is included in Eq. (A3).

-
- [1] S. Braunstein and P. van Loock, *Rev. Mod. Phys.* **77**, 513 (2005).
- [2] S. Lloyd and S. L. Braunstein, in *Quantum Information with Continuous Variables* (Springer, Dordrecht, 1999), pp. 9–17.
- [3] G. Adesso, S. Ragy, and A. R. Lee, *Open Syst. Inf. Dyn.* **21**, 1440001 (2014).
- [4] A. P. Lund, A. Laing, S. Rahimi-Keshari, T. Rudolph, J. L. O'Brien, and T. C. Ralph, *Phys. Rev. Lett.* **113**, 100502 (2014).
- [5] L.-M. Duan, G. Giedke, J. I. Cirac, and P. Zoller, *Phys. Rev. Lett.* **84**, 2722 (2000).
- [6] S.-Y. Lee, S.-W. Ji, H.-J. Kim, and H. Nha, *Phys. Rev. A* **84**, 012302 (2011).
- [7] C. Navarrete-Benlloch, R. García-Patrón, J. H. Shapiro, and N. J. Cerf, *Phys. Rev. A* **86**, 012328 (2012).
- [8] M. Walschaers, C. Fabre, V. Parigi, and N. Treps, *Phys. Rev. A* **96**, 053835 (2017).
- [9] R. Horodecki, P. Horodecki, M. Horodecki, and K. Horodecki, *Rev. Mod. Phys.* **81**, 865 (2009).
- [10] R. Renner, *Int. J. Quantum. Inf.* **06**, 1 (2008).
- [11] S. Pirandola, J. Eisert, C. Weedbrook, A. Furusawa, and S. L. Braunstein, *Nat. Photonics* **9**, 641 (2015).
- [12] M. S. Zubairy, *Quantum Mechanics for Beginners: With Applications to Quantum Communication and Quantum Computing* (Oxford University Press, Oxford, 2020).
- [13] Y. Maleki, *Eur. Phys. J. Plus* **136**, 1028. (2021)..
- [14] W. Ge, K. Jacobs, S. Asiri, M. Foss-Feig, and M. S. Zubairy, *Phys. Rev. Res.* **2**, 023400 (2020).
- [15] S. Barnett, *Quantum Information*, Oxford Master Series in Physics Vol. 16 (Oxford University Press, Oxford, 2009).
- [16] M. Genovese, *Phys. Rep.* **413**, 319 (2005).
- [17] G. Giedke and J. I. Cirac, *Phys. Rev. A* **66**, 032316 (2002).
- [18] J. Fiurášek, *Phys. Rev. Lett.* **89**, 137904 (2002).
- [19] G. S. Agarwal and K. Tara, *Phys. Rev. A* **43**, 492 (1991).
- [20] A. Ourjoumteev, F. Ferreyrol, R. Tualle-Brouiri, and P. Grangier, *Nat. Phys.* **5**, 189 (2009).
- [21] A. Zavatta, S. Viciani, and M. Bellini, *Science* **306**, 660 (2004).
- [22] A. Ourjoumteev, A. Dantan, R. Tualle-Brouiri, and P. Grangier, *Phys. Rev. Lett.* **98**, 030502 (2007).
- [23] S. L. Zhang, Y. L. Dong, X. B. Zou, B. S. Shi, and G. C. Guo, *Phys. Rev. A* **88**, 032324 (2013).
- [24] A. Zavatta, V. Parigi, M. S. Kim, H. Jeong, and M. Bellini, *Phys. Rev. Lett.* **103**, 140406 (2009).
- [25] V. Parigi, A. Zavatta, M. Kim, and M. Bellini, *Science* **317**, 1890 (2007).
- [26] T. Opatrný, G. Kurizki, and D.-G. Welsch, *Phys. Rev. A* **61**, 032302 (2000).
- [27] L. Hu, Z. Liao, and M. S. Zubairy, *Phys. Rev. A* **95**, 012310 (2017).
- [28] Y. Yang and F.-L. Li, *Phys. Rev. A* **80**, 022315 (2009).
- [29] S. L. Zhang and P. van Loock, *Phys. Rev. A* **84**, 062309 (2011).
- [30] J. Fiurášek, *Phys. Rev. A* **84**, 012335 (2011).
- [31] F. Dell'Anno, S. De Siena, and F. Illuminati, *Phys. Rev. A* **81**, 012333 (2010).
- [32] F. Dell'Anno, S. De Siena, L. Albano, and F. Illuminati, *Phys. Rev. A* **76**, 022301 (2007).
- [33] J. Wenger, R. Tualle-Brouiri, and P. Grangier, *Phys. Rev. Lett.* **92**, 153601 (2004).
- [34] A. I. Lvovsky and J. Mlynek, *Phys. Rev. Lett.* **88**, 250401 (2002).
- [35] M. O. Scully and M. S. Zubairy, *Quantum Optics* (Cambridge University Press, Cambridge, 1997).
- [36] M. A. Taylor and W. P. Bowen, *Phys. Rep.* **615**, 1 (2016).
- [37] G. S. Agarwal, *Quantum Optics* (Cambridge University Press, Cambridge, 2012).
- [38] X.-x. Xu, *Phys. Rev. A* **92**, 012318 (2015).
- [39] M. Mičuda, O. Haderka, and M. Ježek, *Phys. Rev. A* **78**, 025804 (2008).
- [40] M. J. Fitch, B. C. Jacobs, T. B. Pittman, and J. D. Franson, *Phys. Rev. A* **68**, 043814 (2003).
- [41] K. Sanaka, K. J. Resch, and A. Zeilinger, *Phys. Rev. Lett.* **96**, 083601 (2006).

- [42] K. J. Resch, J. L. O'Brien, T. J. Weinhold, K. Sanaka, and A. G. White, *Phys. Rev. Lett.* **98**, 203602 (2007).
- [43] S.-Y. Lee and H. Nha, *Phys. Rev. A* **82**, 053812 (2010).
- [44] A. Biswas and G. S. Agarwal, *Phys. Rev. A* **75**, 032104 (2007).
- [45] N. Biagi, L. S. Costanzo, M. Bellini, and A. Zavatta, *Phys. Rev. Lett.* **124**, 033604 (2020).
- [46] T. Das, R. Prabhu, A. Sen(De), and U. Sen, *Phys. Rev. A* **93**, 052313 (2016).
- [47] Y. Maleki and M. S. Zubairy, *Phys. Rev. A* **105**, 032428 (2022).
- [48] J. W. Noh, A. Fougères, and L. Mandel, *Phys. Rev. Lett.* **67**, 1426 (1991).
- [49] Y. Chen, J. D. Müller, P. T. So, and E. Gratton, *Biophys. J.* **77**, 553 (1999).
- [50] G. Zambra, A. Andreoni, M. Bondani, M. Gramegna, M. Genovese, G. Brida, A. Rossi, and M. G. A. Paris, *Phys. Rev. Lett.* **95**, 063602 (2005).